nature synthesis

Article

https://doi.org/10.1038/s44160-023-00353-z

Radical thioesterification via nickel-catalysed sensitized electron transfer

Received: 22 November 2022

Accepted: 22 May 2023

Published online: 10 July 2023

Check for updates

Huamin Wang[1,4], Zhao Liu[2,4], Ankita Das[1], Peter Bellotti[1], Sebastian Megow[3], Friedrich Temps[3] ✉, Xiaotian Qi[2] ✉ & Frank Glorius[1] ✉

Multi-catalytic reaction modes have attracted widespread attention in synthetic chemistry. The merger of nickel catalysis with photoredox catalysis has offered a powerful platform for synthesis of molecules with attractive properties. Nonetheless, the conceptual development of nickel-catalysed, sensitized electron transfer is of pivotal relevance, but is still greatly limited. Here we describe the development of a radical cross-thioesterification process by nickel-catalysed sensitized electron transfer. The strategy can produce diverse methyl thioesters, which are not only found in natural products, materials and pharmaceuticals but also are widespread precursors in synthetic chemistry and biological processes. This catalytic mode features high chemoselectivity, good functional group tolerance and excellent scalability. Perhaps more important was the finding that various drugs and amino acids were successfully functionalized in this system. Experimental studies, nanosecond transient spectroscopic analysis, and density functional theory calculations reveal that the merger of photocatalytic electron transfer, energy transfer and nickel catalysis plays an essential role in this radical thioesterification reaction.

The development of effective and logical strategies that sustainably access valuable and challenging molecules from simple feedstocks is one of the central tenets of modern synthetic chemistry, as well as relentless pursuit of chemists. Methyl thioesters not only are found in natural products and drug molecules but also represent important synthetic precursors in biosyntheses, such as the native chemical ligation reactions towards increasingly large polypeptides and proteins (Fig. 1a)[1–6]. Classical approaches to forging methyl thioester moieties generally rely on multistep syntheses or substitution reactions between electrophilic acyl compounds with either nucleophilic sodium methylthiolate or methyl mercaptan[7–9]. Nonetheless, these methods are plagued by the undesirable chemical properties of these two nucleophiles (Fig. 1b). Specifically, the handling of gaseous methyl mercaptan is not operationally straightforward, and sodium methylthiolate hydrolyses in moist air to the former compound. In addition to require of non-ideal reagents, other synthetic challenges such as extra preparatory steps of the starting materials, narrow functional group compatibility and harsh reaction conditions have severely curbed the efficient construction of valuable methyl thioesters through classical methods[10–14]. To address these liabilities, the Wu group successfully developed a palladium-catalysed carbonylation–thiomethylation of aryl halides with CO and thioesters[15]. In summary, reported methods can form limited thioesters, but methyl thioesters remain challenging to synthesize. Thus, broadly substrate-compatible, easy-to-operate and biocompatible strategies for methyl thioesters are yet underdeveloped but in high demand.

Over the past decade, radical reactions triggered by photocatalysis have provided a powerful and efficient platform for the construction of challenging molecules[16–38]. In this field, the combination of transition metal catalysis for bond formation with photoinduced electron- and/or energy transfer processes has attracted increasing attention (Fig. 1c)[39–41]. Nickel-catalysed, photoinduced electron transfer (ET) strategies have been deeply investigated and successfully applied to synthetic chemistry[42–50]. Moreover, the amalgamation of energy transfer catalysis

[1]Organisch-Chemisches Institut, Westfälische Wilhelms-Universität Münster, Münster, Germany. [2]College of Chemistry and Molecular Sciences, Wuhan University, Wuhan, China. [3]Institute of Physical Chemistry, Christian-Albrechts-University Kiel, Kiel, Germany. [4]These authors contributed equally: Huamin Wang, Zhao Liu. ✉e-mail: temps@phc.uni-kiel.de; qi7xiaotian@whu.edu.cn; glorius@uni-muenster.de

https://doi.org/10.1038/s44160-023-00353-z

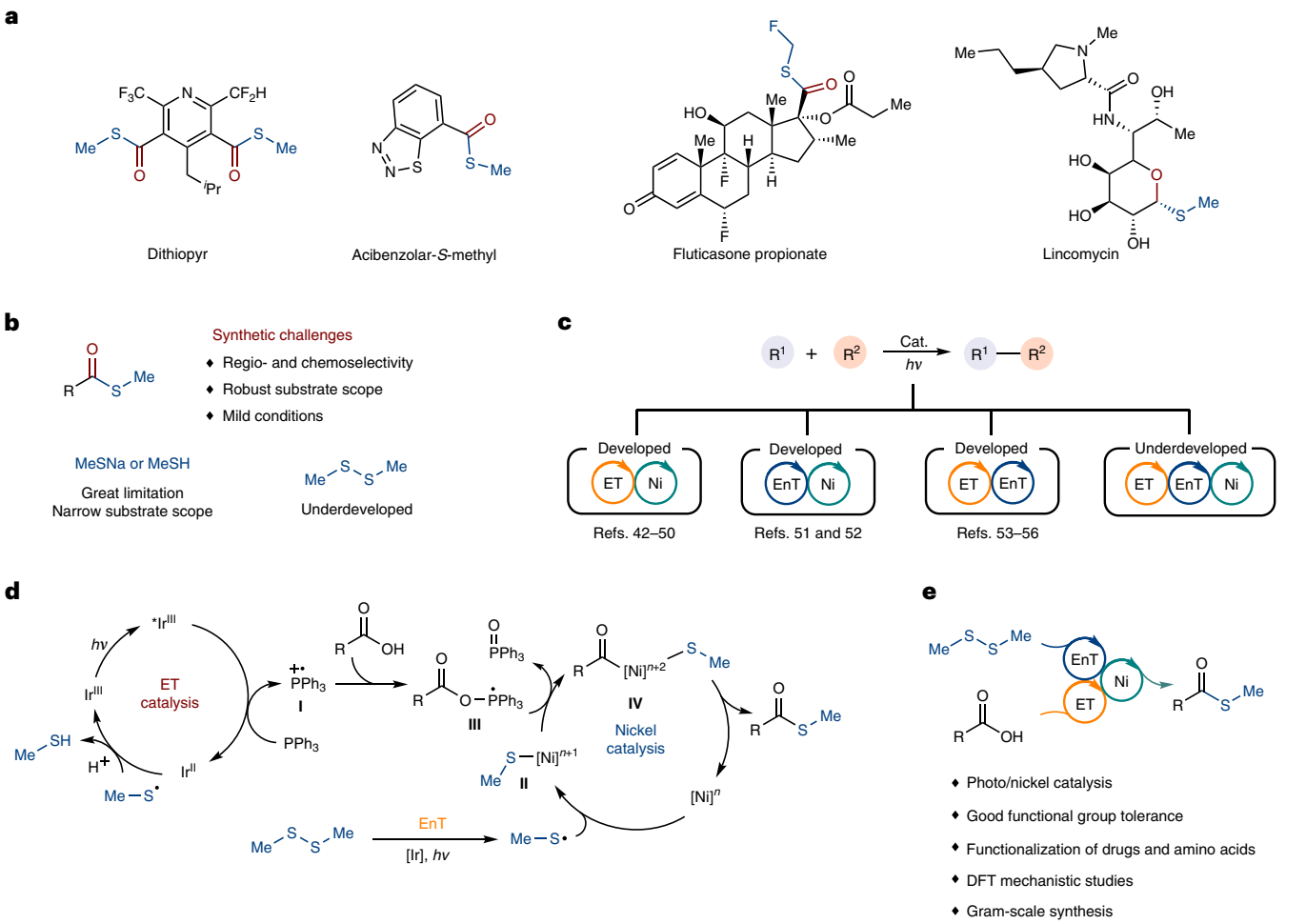

Fig. 1 | Development of a strategy for the synthesis of thiomethyl esters. **a**, Representative biologically active thiomethyl esters. **b**, Synthetic challenges of methyl thioesters. **c**, Synergistic mode of photocatalysis and nickel catalysis. **d**, Working hypothesis. **e**, This work: nickel-catalysed, sensitized ET radical methyl thioesterification. Ni, nickel-catalysed process; PPh_3, triphenylphosphine; [Ir] and Ir, Ir[dF(CF_3)ppy$_2$(dtbbpy)][PF_6]; *hν*, visible light irradiation; cat., catalysis.

(EnT) with nickel catalysis has offered new opportunities for organic cross-coupling reactions (Fig. 1c). Energy transfer-mediated nickel catalysis for the construction of C–O and C–C bonds was pioneered by the groups of MacMillan[51] and Molander[52], respectively. Intriguingly, successful combination of photoinduced energy transfer process (EnT) with ET process by Xiao[53], König[54], Gilmour[55], Weaver[56] and their co-workers paved the way to new radical reaction scenarios (Fig. 1c). So far, only a few examples that operate through ET/nickel catalysis followed by single electron transfer (SET) have been reported by Rueping[57] and Chu[58], successfully enabling the generation of tri-substituted alkenes via a three-component cross-coupling reaction (Fig. 1c). In this type of reactions, energy transfer from excited photocatalysts often plays a role in the last step, enabling alkene isomerizations[57,58]. Nevertheless, more attractive roles for energy transfer in multi-catalytic mode remain to be exploited. For instance, energy transfer with a photosensitizer can promote chemical bond cleavage[17,59,60], which offers more possibilities for constructing functional molecules.

Considering the importance and abundance of carboxylic acids in nature and the easy availability of dimethyl disulfide (DMDS), construction of thiomethyl esters from these two starting materials is an attractive strategy. In this Article, to address the synthetically challenging methyl thioesterification of carboxylic acids, we envisioned that merging energy transfer with ET could offer a cooperative manifold with nickel catalysis. According to the hypothesis, we designed a possible catalytic process (Fig. 1d). Thiomethyl radical, formed from DMDS via photocatalytic energy transfer[60], would react with a nickel catalyst to form nickel complex (**II**). In this system, an active phosphorus radical cation might be generated via photocatalytic ET, as described by Doyle and co-workers[61]. Subsequently, nucleophilic attack of carboxylic acids produces the intermediate **III**. Then, acyl nickel complex (**IV**) would be obtained via the interaction of intermediate **II** with **III**. Further reductive elimination of **IV** would forge the desired product. Herein we describe the successful merger of a nickel-catalysed, energy transfer and ET for the radical thiomethyl esterification of carboxylic acids (Fig. 1e).

Results and discussion

Evaluation of the reaction conditions

To evaluate this multi-catalytic hypothesis, 4-phenylbutyric acid (**1**) and DMDS (**2**) were chosen as reaction partners. Pleasingly, after extensive optimization, 95% yield of thiomethyl ester (**3**) could be obtained with $NiBr_2$(diglyme) and Ir[dF(CF_3)ppy$_2$(dtbbpy)][PF_6] [Ir-F] as co-catalysts, triphenylphosphine (PPh_3) and pyridine as additives (Fig. 2a, entry 1). It is worth mentioning that no decarboxylation by-product was observed in this reaction system, which shows high chemoselectivity[62,63]. The effect of other essential reaction parameters was further investigated (Fig. 2a). Noteworthily, the reaction yield dropped substantially in the absence of nickel catalyst (Fig. 2a, entry 2). Similarly, no desired product was observed without either photocatalyst or irradiation under visible light (Fig. 2a, entry 3). Further screening revealed that PPh_3 plays an essential role in this transformation (Fig. 2a, entry 4). In addition, 80% yield of product was obtained in the absence of pyridine (Fig. 2a,

https://doi.org/10.1038/s44160-023-00353-z

a

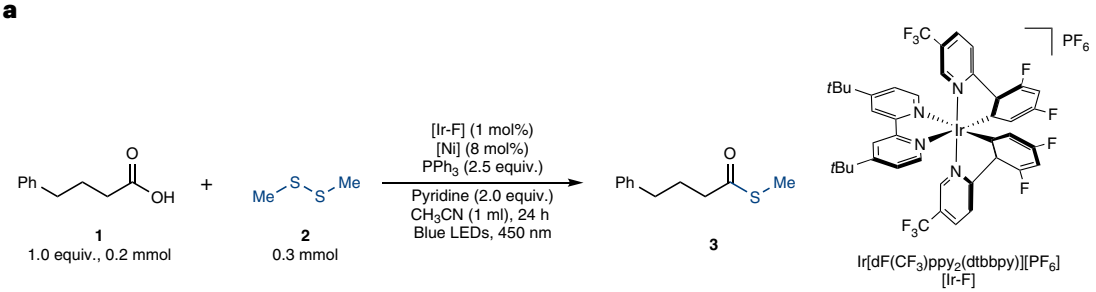

Entry	Variation from the standard conditions	Yield (%) of **3**[a]
1	None	95 (92)
2	Without $NiBr_2$(diglyme)	Trace
3	Without [Ir-F] or *hv*	ND
4	Without PPh_3	ND
5	Without pyridine	80
6	PPh_3 (1.0 equiv.)	20
7	PPh_3 (3.0 equiv.)	95
8	**2** (0.2 mmol)	76
9	**2** (0.4 mmol)	82
10	$NiBr_2$(diglyme) (15 mol%)	42
11	$NiBr_2$(diglyme) (4 mol%)	82
12	$Ni(OTf)_2$	65
13	$NiCl_2$	59

b

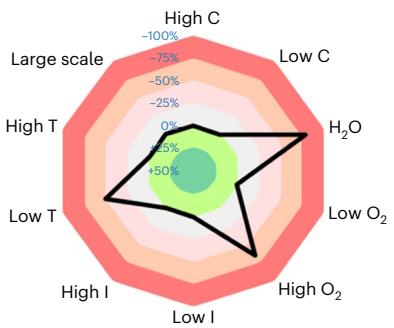

c

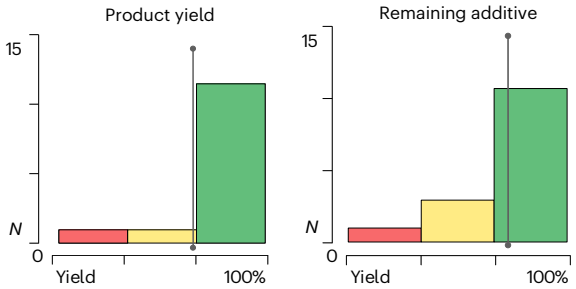

Fig. 2 | Investigation of reaction parameters. a, Effect of the reaction parameters, conditions: **1** (0.2 mmol, 1.0 equiv.), **2** (0.3 mmol, 1.5 equiv.), [Ir-F] (1 mol%), Ni catalyst (8 mol%), PPh_3 (2.5 equiv.), pyridine (2.0 equiv.), and CH_3CN (1 ml), argon, 450 nm, 24 h. ^1H NMR spectroscopic yield with dibromomethane as internal standard. Isolated yield is given in parentheses. LED, light-emitting diode; ND, not detected. **b**, Sensitivity assessment for high levels of reproducibility. **c**, Additive-based robustness screen for the test of functional group tolerance.

entry 5). Increasing the amount of PPh_3 did not affect the reaction yield, while the yield dropped substantially when less PPh_3 was used (Fig. 2a, entries 6 and 7). Moreover, changing the amount of DMDS had no obvious effect on the reaction efficiency (Fig. 2a, entries 8 and 9). Higher or lower amount of the nickel catalyst led to low reaction yields (Fig. 2a, entries 10 and 11). Additionally, other nickel catalysts could also work for this protocol, albeit with lower efficiency (Fig. 2a, entries 12 and 13).

Sensitivity assessment

A condition-based sensitivity screening approach was carried out (Fig. 2b)[64], which demonstrates that the reaction of synthesizing compound **3** is sensitive to high oxygen concentration, low temperature and water content. Pleasingly, good efficiency of this transformation was observed at high temperature and light intensities (Supplementary Section 4).

Additive-based robustness screen

The robustness and the functional group tolerance of this radical two-component thioesterification protocol were investigated by applying an intermolecular additive-based screening method[65]. Most of the examined additives could be well tolerated, and high reaction yields were observed. These findings highlight the remarkable mildness and tolerance of our methodology (Fig. 2c and Supplementary Section 5).

Mechanistic investigations

To provide mechanistic details to support the proposed catalytic cycle, Stern–Volmer luminescence quenching experiments were carried out. As shown in Fig. 3a, the excited photocatalyst could be quenched by either the PPh_3 or DMDS (**2**), which supports our hypothesis. Additionally, UV/Vis absorption experiments were

https://doi.org/10.1038/s44160-023-00353-z

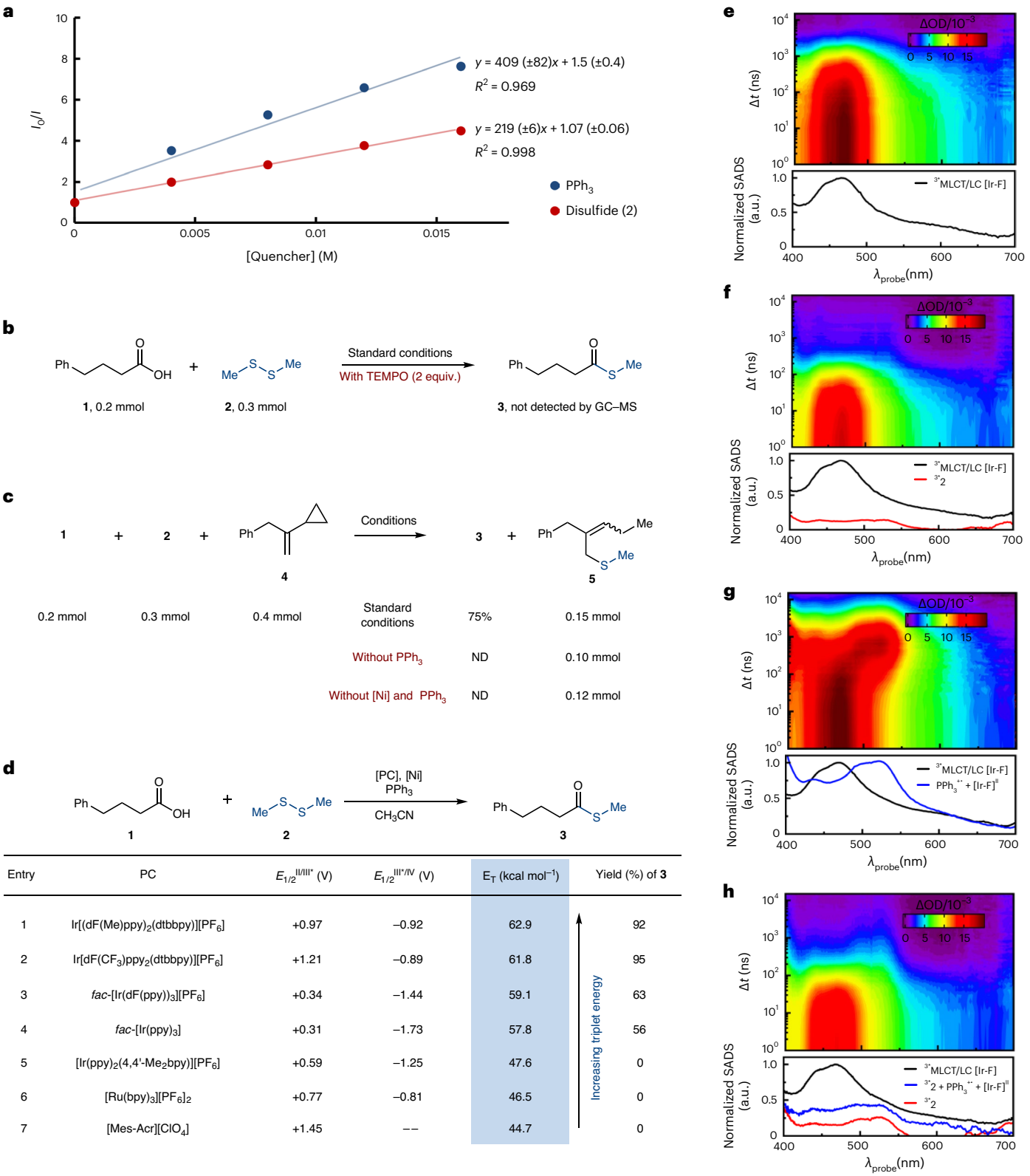

Entry	PC	$E_{1/2}^{II/III*}$ (V)	$E_{1/2}^{III*/IV}$ (V)	E_T (kcal mol^{-1})	Yield (%) of **3**
1	Ir[(dF(Me)ppy)$_2$(dtbbpy)][PF$_6$]	+0.97	−0.92	62.9	92
2	Ir[dF(CF$_3$)ppy$_2$(dtbbpy)][PF$_6$]	+1.21	−0.89	61.8	95
3	*fac*-[Ir(dF(ppy))$_3$][PF$_6$]	+0.34	−1.44	59.1	63
4	*fac*-[Ir(ppy)$_3$]	+0.31	−1.73	57.8	56
5	[Ir(ppy)$_2$(4,4′-Me$_2$bpy)][PF$_6$]	+0.59	−1.25	47.6	0
6	[Ru(bpy)$_3$][PF$_6$]$_2$	+0.77	−0.81	46.5	0
7	[Mes-Acr][ClO$_4$]	+1.45	––	44.7	0

Increasing triplet energy

Fig. 3 | Mechanistic investigations for the synthesis of thiomethyl esters by this protocol. a, Stern–Volmer fluorescence quenching analysis. **b**, Radical inhibitor and probe experiments. **c**, Control experiments. **d**, Comparison of various triplet sensitizers. **e**, Transient spectroscopy of [Ir-F]. **f**, Transient spectroscopy of [Ir-F] with DMDS (**2**). **g**, Transient spectroscopy of [Ir-F] with PPh_3. **h**, Transient spectroscopy of [Ir-F] with **2** and PPh_3. GC–MS, gas chromatography–mass spectrometer; PC, photocatalyst.

also performed (Supplementary Fig. 5). Then, this multi-catalytic process was completely inhibited in the presence of TEMPO (tetramethylpiperidine-1-oxyl), revealing that a radical process might be involved (Fig. 3b). Thiomethyl radical was trapped by the (2-cyclopropylallyl)benzene (**4**), and no acyl radical **8** was observed. This probe experiment further suggests the intermediacy of radical

in this system (Fig. 3c). Subsequently, control experiments show that the sulfur radical could be formed from DMDS (**2**) in absence of nickel catalyst or PPh_3 (Fig. 3c). Furthermore, various triplet sensitizers were evaluated (Fig. 3d). The yield of the methylthiolated product correlates to the triplet energy rather than the redox potential of the photocatalysts, which means that the production of thiomethyl radicals from disulfides is probably promoted by EnT[60,66].

Transient absorption spectroscopic studies

Nanosecond transient electronic absorption spectroscopy (ns-TEAS) was employed to obtain further insight into the kinetics of the initial activation of PPh_3 and DMDS (**2**) by the [Ir-F] (Fig. 3 and Supplementary Section 6.7). The ns-TEAS results of the sole [Ir-F] as well as mixtures of [Ir-F] with DMDS **2**, [Ir-F] with PPh_3, and [Ir-F] with DMDS **2** and PPh_3 in Ar-saturated MeCN upon excitation at λ_{exc} = 387 nm are displayed in Fig. 3. Global and target analysis of the data was performed using the python package KiMoPack, which yielded the species-associated difference spectra (SADS, bottom panel)[67]. The pure [Ir-F] (Fig. 3e) exhibits a broad excited state absorption band peaking at λ_{probe} = 465 nm, which is ascribed to the triplet metal-to-ligand charge-transfer/ligand-centred (^{3}*MLCT/LC) state of the photocatalyst[60]. Addition of **2** to the solution (Fig. 3f) leads to a notable shortening of the ^{3}*MLCT/LC lifetime and to the formation of a second species with distinct absorption peaks at λ_{probe} = 400, 440 nm that has previously been assigned to the triplet state of **2** (^{3}*__2__), which is generated from triplet–triplet energy transfer[60,68]. The mixture of [Ir-F] and PPh_3 (Fig. 3g) shows the accelerated depletion of the ^{3}*MLCT/LC state of the photosensitizer in favour of a species with a broad absorption band centred at λ_{probe} = 520 nm indicates the excited state ET leading to the formation of the radical cation $PPh_3^{+\bullet}$ as well as to the reduction of the ([Ir-F]^{II}) photosensitizer[67–71]. The mixture of all three compounds (Fig. 3h) mostly resembles the photodynamics resulting from excited state ET between the [Ir-F] and **2**. However, some superimposed triplet–triplet energy transfer contribution caused by the interaction of the photocatalyst with PPh_3 can be identified from the decomposed spectra. In summary, the ns-TEAS results provide evidence that the initial activation of the PPh_3 to $PPh_3^{+\bullet}$ is due to one-electron oxidation from the ^{3}*MLCT/LC state of the photocatalyst and that the previously observed TTEnT between the photocatalyst and the disulfide (**2**) also occurs in the presence of PPh_3.

DFT studies

To gain more mechanistic insights, density functional theory (DFT) calculations were performed to investigate the radical methyl thioesterification of carboxylic acids. Firstly, computational studies suggest that the activation of PPh_3 through the single ET from thiomethyl radical is endergonic by 28.9 kcal mol^{-1} (Supplementary Fig. 11), indicating the SET pathway is thermodynamically unfeasible, which further supports the rationality of activation of PPh_3 by excited state photosensitizer[72–75]. With the proposal of the activation of PPh_3 and thiomethyl radicals, we paid attention to the detailed reaction pathway of methyl thioesterification of carboxylic acids, especially the C(acyl)–O activation mechanism.

As shown in Fig. 4a, the combination of carboxylate anion with PPh_3 radical cation, which leads to the formation of complex **7**, is exergonic by 6.9 kcal mol^{-1}. The calculated Mulliken atomic spin population reveals that complex **7** is a phosphorus-centred radical species as the phosphorus atom has the largest spin density (0.55). From **7**, the C(acyl)–O activation can be achieved through the β-scission of phosphorus radical **7** (via **TS-1**), which generates the acyl radical **8** and triphenylphosphine oxide. This metal-free pathway requires an activation free energy of 17.8 kcal mol^{-1}.

In the presence of the nickel catalyst (Fig. 4b), nickel(I) bromide **10** can be used to stabilize the thiomethyl radical by forming a triplet thiomethyl nickel(II) complex ^{3}**11**. The corresponding singlet structure is less stable than the triplet structure by 7.8 kcal mol^{-1}. Subsequently, thiomethyl nickel(II) complex ^{3}**11** can further trap the phosphorus radical **7** and forms a stable doublet nickel complex **12**. As shown in Fig. 4b, most of the spin is located at the nickel centre (0.97). Moreover, natural population analysis (NPA) of **12** reveals that the NPA charge of the [Br-Ni-SMe] fragment is −0.97. These results support that the metal centre in complex **12** is nickel(I). We surmise that the SET between thiomethyl nickel(II) complex and phosphorus radical **7** can occur rapidly, thereby resulting in the single-electron reduction of nickel(II) to nickel(I). The energy barrier of the SET[76] between thiomethyl nickel(II) complex and phosphorus radical **7** is only 0.9 kcal mol^{-1} (Supplementary Section 7), which verifies the facile single-electron reduction of nickel(II) to nickel(I) can occur rapidly. Considering the free energy of nickel(I) complex **12** with respect to **10** is −26.0 kcal mol^{-1}, we can conclude that the successive trapping of thiomethyl radical and phosphorus radical using nickel(I) bromide **10** is thermodynamically feasible and irreversible.

From **12** (Fig. 4b), the C(acyl)–O activation can be achieved through the C–O oxidative addition to the nickel(I) centre (via **TS-2**). The activation free energy is 9.9 kcal mol^{-1}, which is 7.9 kcal mol^{-1} lower than that of **TS-1** in the metal-free C(acyl)–O activation pathway. Subsequent C–S reductive elimination from the acyl nickel(III) complex **13** (via **TS-3**) is demonstrated to be a barrier-less step. The final ligand exchange with two molecular PPh_3 can release the thiomethyl ester product **3** and regenerate the nickel(I) bromide **10**. Besides the metal-free and two-electron oxidative addition mechanisms for C(acyl)–O activation, Ni(I)-mediated radical C(acyl)–O activation mechanism has also been considered in DFT calculation (Fig. 4c). An open-shell singlet transition state **TS-4** containing a three-membered cyclic core structure was located. Vibrational frequency calculation and intrinsic reaction coordinate calculation of **TS-4** suggest that this process is analogous to nickel(I)-mediated β-scission of phosphorus radical. However, the higher activation free energy (26.2 kcal mol^{-1}) indicates this radical pathway is disfavoured. Therefore, the radical methyl thioesterification of carboxylic acids prefers to occur through successive radical trapping with nickel(I) complex, C(acyl)–O oxidative addition, and C–S reductive elimination. The nickel catalyst plays a critical role in tuning the stability and reactivity of different radical species and promoting the C(acyl)–O activation.

Scope for thioesterification

Subsequently, we examined the substrate scope under the optimal condition (Tables 1 and 2). Firstly, primary carboxylic acids were evaluated in their reactions with DMDS (**2**) (Table 1). Good yields of the corresponding products were observed under standard condition (**3** and **15**–**18**, 50–92% yields). Additionally, secondary carboxylic acids were tested (**19**–**25**, 56–92% yields). The substrates containing electron-rich aromatic ring (**19**, 56% yield), keto group (**23**, 60% yield) and cyclic alkyl groups (**21**, **22**, **24**, 68–92% yields) were compatible with this radical system. Importantly, tertiary carboxylic acids could also react smoothly with DMDS (**2**) to offer desired products in moderate to good yields (**26**–**28**, 54–78% yields), exemplifying the generality of this methyl thioesterification protocol. Then, aryl carboxylic acids with either electron-donating groups (**30**–**32**, **36**, **37**, 60–75% yields) or electron-withdrawing groups (**34** and **35**, 50% and 67% yields, respectively) on the aromatic ring were successfully converted to thiomethyl esters. It is worth mentioning that the efficiency of the reaction was not impeded by ortho substituents on the aromatic ring (**38** and **39**, 60% and 50% yields, respectively). The transformation of heterocyclic carboxylic acids successfully occurred (**40**–**44**, 57–91% yields). With respect to disulfides as coupling partners, thiophene (**45**, 98% yield), aryl (**46** and **47**, 90% and 96% yield, respectively) and alkyl disulfides (**49**–**51**, 69–73% yields, respectively) were also amenable to this reaction, providing the corresponding products in good to

https://doi.org/10.1038/s44160-023-00353-z

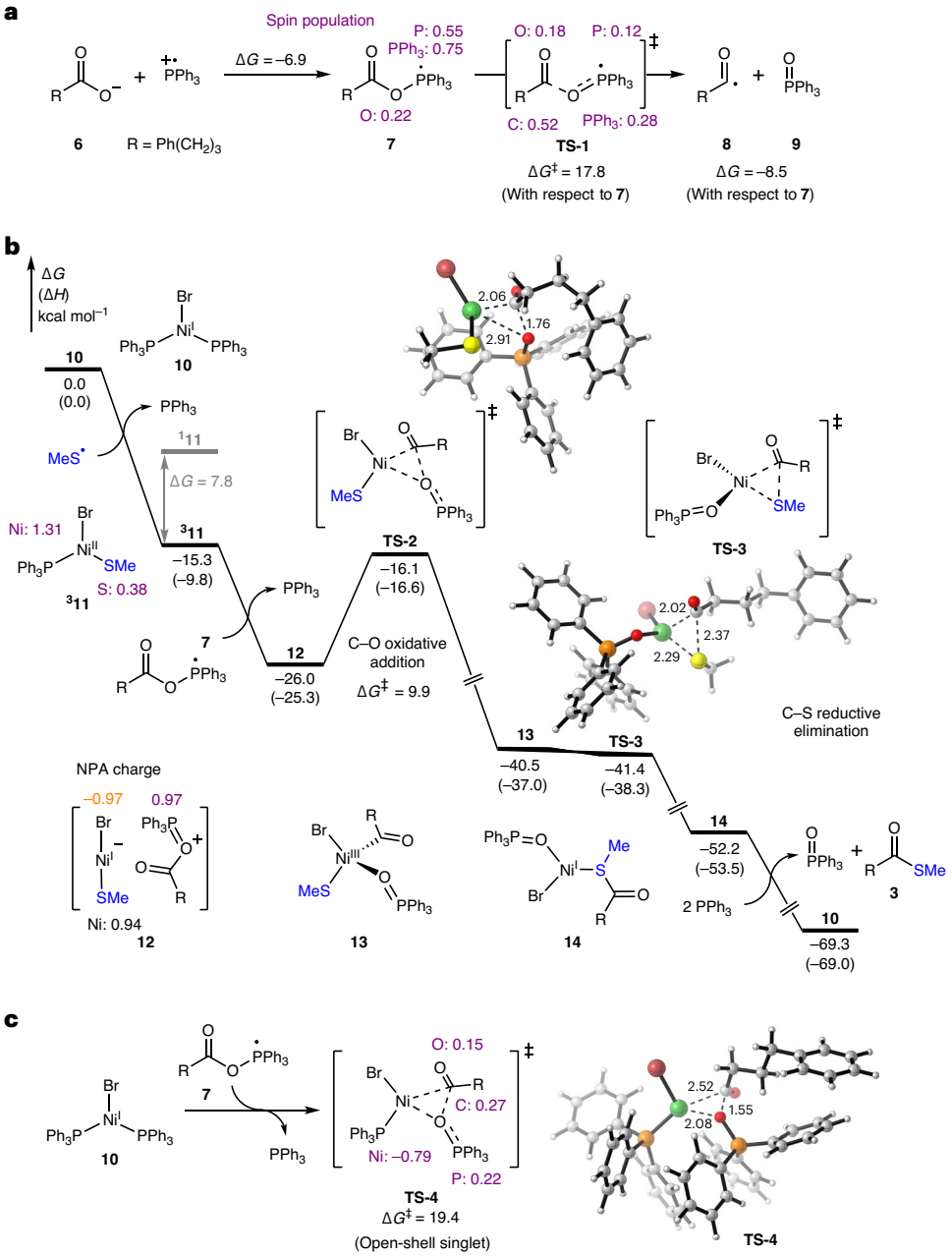

Fig. 4 | DFT studies for this photochemical nickel-catalysed synthesis of thiomethyl esters. a, Metal-free C(acyl)–O activation through the β-scission of phosphorus-centred radical **7**. **b**, Free energy profile of Ni-promoted radical methyl thioesterification of carboxylic acids. **c**, Ni(I)-mediated C(acyl)–O activation in phosphorus radical **7**. The purple numbers denote the Mulliken atomic spin densities at certain atoms. All energies were in kcal mol^{-1} and were calculated at the M06/6-311 + G(d,p)-SDD/SMD(acetonitrile)//B3LYP-D3(BJ)/6-31G(d)-LANL2DZ level of theory. The bond lengths shown in 3D structures are in angstrom. R = Ph(CH$_2$)$_3$.

excellent yields and highlighting the utility of this thioesterification protocol. Pleasingly, *sec*-butyl disulfide and isopropyl disulfide could react well with 4-phenylbutyric acid (**1**) to forge compounds **52** and **53** in 86% and 95% yields, respectively. Unfortunately, in the case of sterically demanding disulfides, such as *tert*-butyl disulfide, no corresponding product was obtained.

Scope for drugs and amino acids

Encouraged by the above results, drug molecules containing the carboxylic group and amino acids were examined. As shown in Table 2, a series of non-steroidal anti-inflammatory drugs, such as ibuprofen (**54**, 70% yield), ketoprofen (**55**, 86% yield), flurbiprofen (**56**, 73% yield), zaltoprofen (**57**, 80% yield) and loxoprofen (**58**, 70% yield) could react with DMDS (**2**) to give the desired products in good yields. Interestingly, citronellic acid was also compatible with this system, offering the desired product in 50% yield (**59**). The drug, containing primary carboxylic acid, was well tolerated (**60**, 76% yield). Probenecid, which is mainly used to treat gout and hyperuricaemia, was converted to its thiomethyl ester in 69% yield (**61**). Additionally, various α-, β- and γ-amino acids were evaluated under the standard condition. Thiomethylated products could be obtained using Boc-protected (**62**, 65% yield) and Cbz-protected (**63**–**65**, 52%, 74%, 83% yields) α-amino acids as reaction partners. β-Amino acids featuring azetidine (**67**), piperidine (**69**) and pyrrolidine (**70**) rings were introduced in this protocol, and delivered the corresponding products in 60–85% yields. The successful reactions of other β-amino

https://doi.org/10.1038/s44160-023-00353-z

Table 1 | Scope for thioesterification

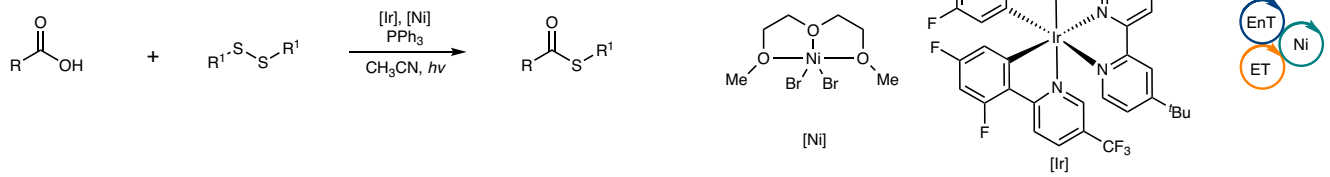

Primary carboxylic acids

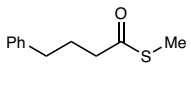

3, 92%

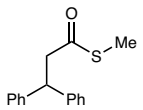

15, 70%

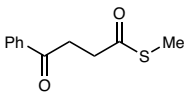

16, 50%

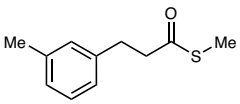

17, 85%

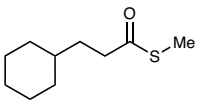

18, 89%

Secondary carboxylic acids

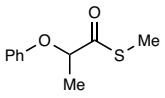

19, 56%

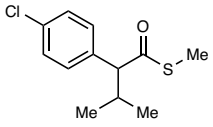

20, 75%

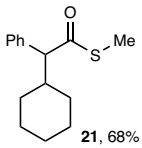

21, 68%

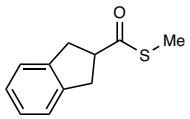

22, 92%

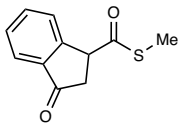

23, 60%

Tertiary carboxylic acids

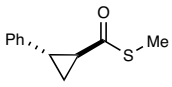

24, (±) 89%

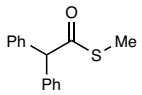

25, 73%

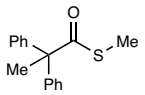

26, 60%

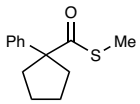

27, 78%

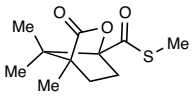

28, 54%

Aryl carboxylic acids

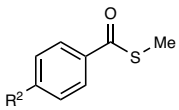

R^2 = Ph, **29**, 66%
R^2 = OMe, **30**, 65%
R^2 = OCF_3, **31**, 75%
R^2 = ^{n}Bu, **32**, 63%
R^2 = 2-Pyridyl, **33**, 72%

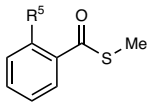

R^5 = SMe, **38**, 60%
R^5 = Cl, **39**, 50%

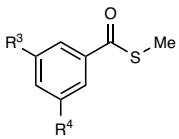

R^3 = Br, R^4 = H, **34**, 50%
R^3 = CF_3, R^4 = H, **35**, 67%
R^3 = Me, R^4 = H, **36**, 62%
R^3 = Me, R^4 = Me, **37**, 60%

Heterocyclic carboxylic acids

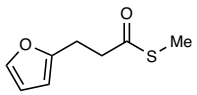

40, 91%

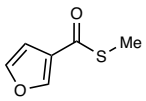

41, 62%

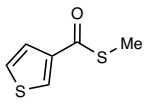

42, 67%

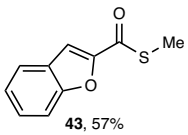

43, 57%

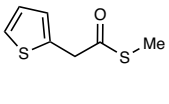

44, 79%

Thiophene disulfide

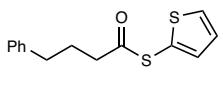

45, 98%

Aryl disulfides

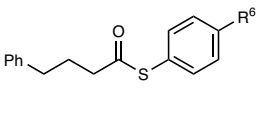

R^6 = OMe, **46**, 90%
R^6 = Cl, **47**, 96%

Benzyl disulfide

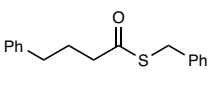

48, 71%

Alkyl disulfide

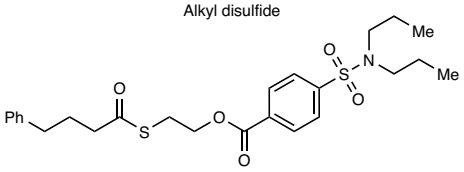

49, 73%[a]

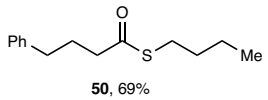

50, 69%

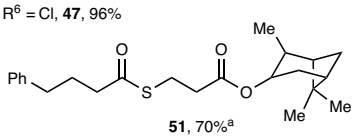

51, 70%[a]

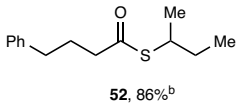

52, 86%[b]

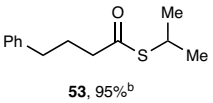

53, 95%[b]

Reaction conditions: unless otherwise noted, isolated yields are reported. Carboxylic acids (0.2 mmol, 1.0 equiv.), DMDS (0.3 mmol, 1.5 equiv.), [Ir-F] (1 mol%), PPh_3 (2.5 equiv.), pyridine (2.0 equiv.), blue LEDs (18 W, 450 nm), and CH_3CN (1 ml), r.t., 24 h under argon. [a]PPh_3 (3.0 equiv.). [b][Ir-F] (2 mol%), disulfide (0.4 mmol), PPh_3 (0.8 mmol) without pyridine. r.t., room temperature. *hv*, visible light irradiation.

acids further demonstrate the functional group tolerance of this radical approach (**68**, **71** and **72**, 46–80% yields). γ-Amino acids could also be successfully reacted, and formed the desired product in 55% yield (**73**), which shows the compatibility of this method with a wide range of amino acids.

Gram-scale synthesis

To evaluate the scalability of this photochemical protocol, selected reactions were carried out on a larger scale (Table 2 and Supplementary Section 8). Probenecid (**74**) and an azetidine-based amino acid (**75**) were used as substrates, respectively. Pleasingly, desired products **61**

https://doi.org/10.1038/s44160-023-00353-z

Table 2 | Scope for drugs and amino acids

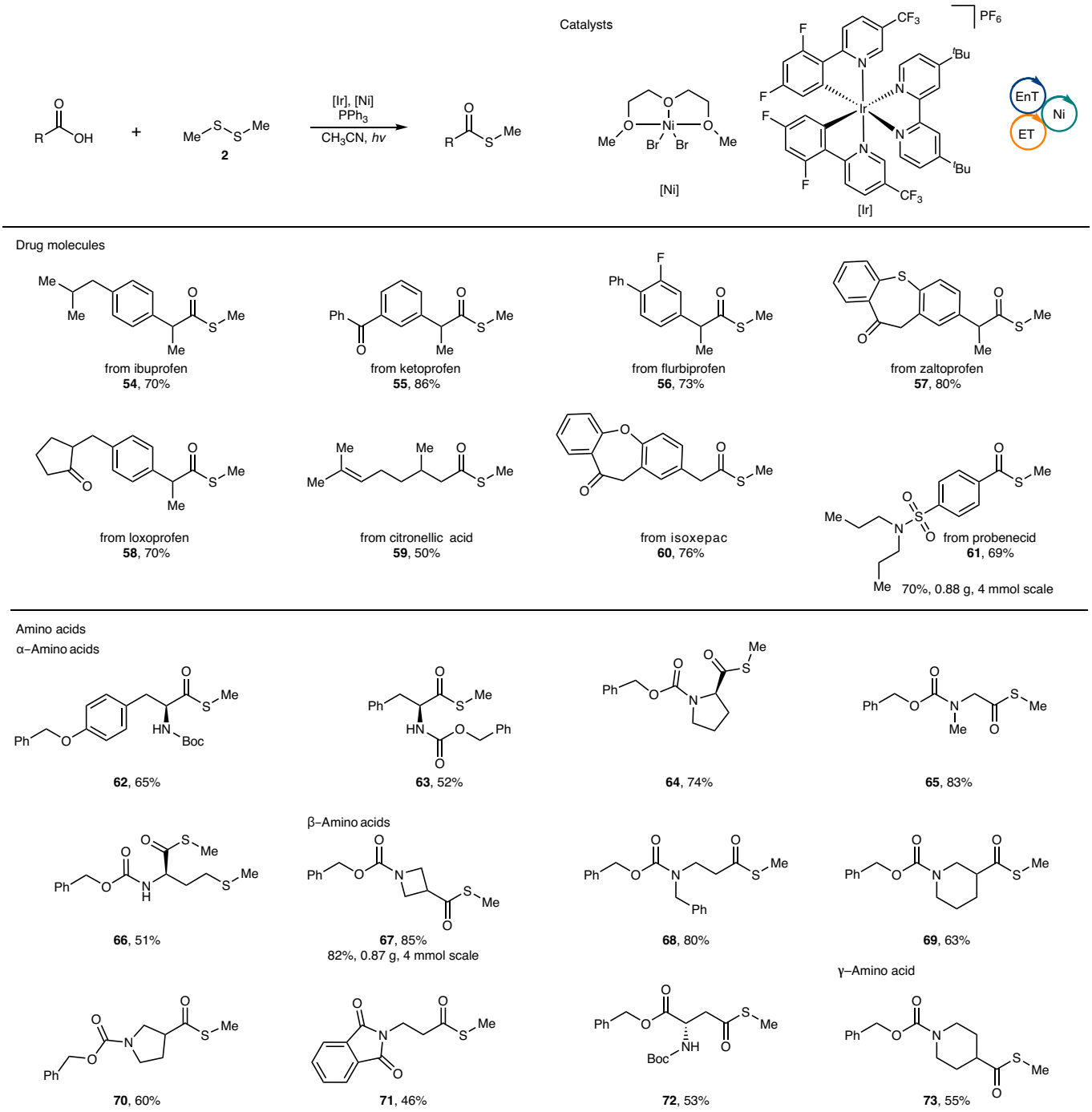

Reaction conditions: unless otherwise noted, isolated yields are reported. Carboxylic acids (0.2 mmol, 1.0 equiv.), DMDS (0.3 mmol, 1.5 equiv.), Ir[dF(CF$_3$)ppy$_2$(dtbbpy)][PF$_6$] (1 mol%), PPh$_3$ (2.5 equiv.), pyridine (2.0 equiv.), blue LEDs (18 W, 450 nm), and CH$_3$CN (1 ml), r.t., 24 h under argon. r.t., room temperature. *hv*, visible light irradiation. Note: configurations for compounds **62**–**64**, **66** and **72** are assumed on the basis of the configurations of the substrates and are unproven.

and **67** could be successfully obtained in 70% yield (0.88 g) and 82% yield (0.87 g), respectively.

Application of product

We next turned our attention to the potential applications of thiomethyl esters (Supplementary Section 9). Compound **61** was submitted to the conditions presented in reported work and provided other valuable compounds[77–79]. For examples, 96% yield of compound **S-76** could be generated via decarbonylation of compound **61**. In addition, alkynylation (**S-77**, 62% yield) and boronation (**S-78**, 92% yield) were also successfully achieved using compound **61** as coupling partner, demonstrating that thiomethyl esters are functional synthetic precursors in a series of chemical transformations.

Conclusion

In summary, we have reported a nickel-catalysed, sensitized ET strategy that features high chemoselectivity, a broad substrate scope, mild reaction conditions and good functional group tolerance. Importantly,

various drugs and amino acids were successfully functionalized using this system. The facile scalability and the synthetic utility of this radical protocol were demonstrated by the gram-scale synthesis and application of products, respectively. Mechanistically, the successful amalgamation of photoinduced ET, energy transfer and nickel catalysis plays an essential role in this two-component radical deoxysulfurization. Therefore, we anticipate that this combination of multiple catalytic systems would have diverse applications in synthetic chemistry and beyond.

Methods

General procedure for synthesis of methyl thioesters

A dried 5 ml Schlenk tube was charged with PPh_3 (0.5 mmol, 2.5 equiv.), carboxylic acid (0.2 mmol, 1.0 equiv.), $NiBr_2$(diglyme) (8 mol%) and Ir[dF(CF_3)ppy$_2$(dtbbpy)][PF_6] (1.0 mol%). Then, reaction mixture was degassed by vacuum-argon purging. After the mixture was thoroughly degassed and filled with argon, the DMDS (**2**, 0.3 mmol, 1.5 equiv.), pyridine (0.4 mmol, 2.0 equiv.) and CH_3CN (1 ml) were added to the vessel under argon atmosphere. Then, the Schlenk tube was sealed tightly and stirred under irradiation with light (λ_{max} = 450 nm) for 24 h. The solvent was removed in vacuo after the reaction. The crude residue was purified by flash column chromatography on silica (*n*-pentane/EtOAc mixtures).

General procedure for synthesis of other thioesters

A dried 5 ml Schlenk tube was charged with PPh_3 (2.5 or 3 equiv.), carboxylic acid (**1**, 0.2 mmol, 1.0 equiv.), $NiBr_2$(diglyme) (8 mol%) and Ir[dF(CF_3)ppy$_2$(dtbbpy)][PF_6] (1.0 mol%). Then, reaction mixture was degassed by vacuum-argon purging. After the mixture was thoroughly degassed and filled with argon, disulfide (0.3 mmol, 1.5 equiv.), pyridine (0.4 mmol, 2.0 equiv.) and CH_3CN (1 ml) were added to the vessel under argon atmosphere. Then, the Schlenk tube was sealed tightly and stirred under irradiation with light (λ_{max} = 450 nm) for 24 h. The solvent was removed in vacuo after the reaction. The crude residue was purified by flash column chromatography on silica (*n*-pentane/EtOAc mixtures). Note: PPh_3 (3.0 equiv.) was necessary with the benzyl and alkyl disulfides as substrates. Compounds **52** and **53** were synthesized by using [Ir-F] (2 mol%), disulfide (0.4 mmol) and PPh_3 (0.8 mmol) without pyridine.

Data availability

The authors declare that the data supporting the findings of this study are available within the paper and its Supplementary Information.

References

1. Agouridas, V. et al. Native chemical ligation and extended methods: mechanisms, catalysis, scope, and limitations. *Chem. Rev.* **119**, 7328–7443 (2019).
2. Kim, J. et al. Site-selective functionalization of methionine residues via photoredox catalysis. *J. Am. Chem. Soc.* **142**, 21260–21266 (2020).
3. Takahashi, N. et al. Reactive sulfur species regulate tRNA methythiolation and contribute to insulin secretion. *Nucleic Acids Res.* **45**, 435–445 (2017).
4. Forouhar, F. et al. Two Fe-S clusters catalyze sulfur insertion by radical-SAM methylthiotransferases. *Nat. Chem. Biol.* **9**, 333–338 (2013).
5. Yang, J., Wang, C., Xu, S. & Zhao, J. Ynamide-mediated thiopeptide synthesis. *Angew. Chem. Int. Ed.* **58**, 1382–1386 (2019).
6. Song, S. et al. DMSO-catalysed late-stage chlorination of (hetero)arenes. *Nat Catal.* **3**, 107–115 (2020).
7. Otten, P. A., Oskam, N. & Gen, A. V. A Horner–Wittig approach to *S*,*N*-ketene acetals: acid-catalyzed hydrolysis of *S*,*N*-ketene acetals to (*S*)-thioesters. *Tetrahedron* **52**, 11095–11104 (1996).
8. Hidenobu, O., Hatsuo, M., Kohichi, K., Kiyoshi, S. & Masaichiro, M. Thioalkoxytributyl- and thioalkoxytriphenylphosphonium salts: preparation and application to the synthesis of thiolesters and unsymmetrical sulfides. *Chem. Pharm. Bull.* **35**, 4473–4481 (1987).
9. Kumar, V. et al. Electrophilic activation of carboxylic anhydrides for nucleophilic acylation reactions. *Synthesis* **50**, 3902–3910 (2018).
10. Xie, S. et al. Cu-catalyzed oxidative thioesterification of aroylhydrazides with disulfides. *J. Org. Chem.* **86**, 739–749 (2021).
11. Azeredo, J. B., Godoi, M., Schwab, R. S., Botteselle, G. V. & Braga, A. L. Synthesis of thiol esters using nano CuO/ionic liquid as an eco-friendly reductive system under microwave irradiation. *Eur. J. Org. Chem.* **2013**, 5188–5519 (2013).
12. Basu, B., Paul, S. & Nanda, A. K. Silica-promoted facile synthesis of thioesters and thioethers: a highly efficient, reusable and environmentally safe solid support. *Green Chem.* **12**, 767–771 (2010).
13. Dan, W. et al. A new odorless one-pot synthesis of thioesters and selenoesters promoted by Rongalite. *Tetrahedron* **66**, 7384–7388 (2010).
14. Meshram, H., Reddy, G. S., Bindu, K. H. & Yadav, J. Zinc promoted convenient and general synthesis of thiol esters. *Synlett* **1998**, 877–878 (1998).
15. Li, Y., Bao, G. & Wu, X.-F. Palladium-catalyzed intermolecular transthioetherification of aryl halides with thioethers and thioesters. *Chem. Sci.* **11**, 2187–2192 (2020).
16. Prier, C. K., Rankic, D. A. & MacMillan, D. W. C. Visible light photoredox catalysis with transition metal complexes: applications in organic synthesis. *Chem. Rev.* **113**, 5322–5363 (2013).
17. Zhou, Q.-Q., Zou, Y.-Q., Lu, L.-Q. & Xiao, W.-J. Visible-light-induced organic photochemical reactions through energy-transfer pathways. *Angew. Chem. Int. Ed.* **58**, 1586–1604 (2019).
18. Wenger, O. S. Proton-coupled electron transfer with photoexcited metal complexes. *Acc. Chem. Res.* **46**, 1517–1526 (2013).
19. Kärkäs, M. D., Porco, J. A. Jr & Stephenson, C. R. J. Photochemical approaches to complex chemotypes: applications in natural product synthesis. *Chem. Rev.* **116**, 9683–9747 (2016).
20. Skubi, K. L., Blum, T. R. & Yoon, T. P. Dual catalysis strategies in photochemical synthesis. *Chem. Rev.* **116**, 10035–10074 (2016).
21. Juliá, F., Constantin, T. & Leonori, D. Applications of halogen-atom transfer (XAT) for the generation of carbon radicals in synthetic photochemistry and photocatalysis. *Chem. Rev.* **122**, 2292–2352 (2022).
22. Ye, J., Ju, T., Huang, H., Liao, L.-L. & Yu, D.-G. Radical carboxylative cyclizations and carboxylations with CO_2. *Acc. Chem. Res.* **54**, 2518–2531 (2021).
23. Li, X.-B. et al. Semiconductor nanocrystals for small molecule activation via artificial photosynthesis. *Chem. Soc. Rev.* **49**, 9028–9056 (2020).
24. Holmberg-Douglas, N. & Nicewicz, D. A. Photoredox-catalyzed C–H functionalization reactions. *Chem. Rev.* **122**, 1925–2016 (2022).
25. Wang, S., Tang, S. & Lei, A. Tuning radical reactivity for selective radical/radical cross-coupling. *Sci. Bull.* **63**, 1006–1009 (2018).
26. Zhang, L. & Meggers, E. Steering asymmetric Lewis acid catalysis exclusively with octahedral metal-centered chirality. *Acc. Chem. Res.* **50**, 320–330 (2017).
27. Zhang, B. & Studer, A. Recent advances in the synthesis of nitrogen heterocycles via radical cascade reactions using isonitriles as radical acceptors. *Chem. Soc. Rev.* **44**, 3505–3521 (2015).
28. Plesniak, M. P., Huang, H.-M. & Procter, D. J. Radical cascade reactions triggered by single electron transfer. *Nat. Rev. Chem.* **1**, 0077 (2017).
29. Wang, H., Tian, Y.-M. & König, B. Energy- and atom-efficient chemical synthesis with endergonic photocatalysis. *Nat. Rev. Chem.* **6**, 745–755 (2022).

30. Keum, H., Jung, H., Jeong, J., Kim, D. & Chang, S. Visible-light induced C(sp^2)–H amidation with an aryl–alkyl σ-bond relocation via redox-neutral radical–polar crossover. *Angew. Chem. Int. Ed.* **60**, 25235–25240 (2021).
31. Li, J., Huang, C.-Y. & Li, C.-J. Two-in-one metallaphotoredox cross-couplings enabled by a photoactive ligand. *Chem* **8**, 2419–2431 (2022).
32. Saha, A. et al. Substrate-rhodium cooperativity in photoinduced ortho-alkynylation of arenes. *Angew. Chem. Int. Ed.* **61**, e202210492 (2022).
33. Cesana, P. T. et al. A biohybrid strategy for enabling photoredox catalysis with low-energy light. *Chem* **8**, 174–185 (2022).
34. Silvi, M. & Melchiorre, P. Enhancing the potential of enantioselective organocatalysis with light. *Nature* **554**, 41–49 (2018).
35. Rossi-Ashton, J. A., Clarke, A. K., Unsworth, W. P. & Taylor, R. J. K. Phosphoranyl radical fragmentation reactions driven by photoredox catalysis. *ACS Catal.* **10**, 7250–7261 (2020).
36. Cheng, Y.-Z., Feng, Z., Zhang, X. & You, S.-L. Visible-light induced dearomatization reactions. *Chem. Soc. Rev.* **51**, 2145–2170 (2022).
37. Fabry, D. C. & Rueping, M. Merging visible light photoredox catalysis with metal catalyzed C–H activations: on the role of oxygen and superoxide ions as oxidants. *Acc. Chem. Res.* **49**, 1969–1979 (2016).
38. Yan, J. et al. Divergent functionalization of aldehydes photocatalyzed by neutral eosin Y with sulfone reagents. *Nat. Commun.* **12**, 7214 (2021).
39. Chan, A. Y. et al. Metallaphotoredox: the merger of photoredox and transition metal catalysis. *Chem. Rev.* **122**, 1485–1542 (2022).
40. Huang, H.-M., Bellotti, Chen, P.-P., Houk, K. N. & Glorius, F. Allylic C(sp^3)–H arylation of olefins via ternary catalysis. *Nat. Synth.* **1**, 59–68 (2022).
41. Levin, M. D., Kim, S. & Toste, F. D. Photoredox catalysis unlocks single-electron elementary steps in transition metal catalyzed cross-coupling. *ACS Cent. Sci.* **2**, 293–301 (2016).
42. Kariofillis, S. K. & Doyle, A. G. Synthetic and mechanistic implications of chlorine photoelimination in nickel/photoredox C(sp^3)–H cross-coupling. *Acc. Chem. Res.* **54**, 988–1000 (2021).
43. Tellis, J. C., Primer, D. N. & Molander, G. A. Single-electron transmetalation inorganoboron cross-coupling byphotoredox/nickel dual catalysis. *Science* **345**, 433–436 (2014).
44. Corcoran, E. B. et al. Aryl amination using ligand-free Ni(II) salts and photoredox catalysis. *Science* **353**, 279–283 (2016).
45. Dorsheimer, J. R., Ashley, M. A. & Rovis, T. Dual nickel/photoredox-catalyzed deaminative cross-coupling of sterically hindered primary amines. *J. Am. Chem. Soc.* **143**, 19294–19299 (2021).
46. Qin, Y., Sun, R., Gianoulis, N. P. & Nocera, D. G. Photoredox nickel-catalyzed C–S cross-coupling: mechanism, kinetics, and generalization. *J. Am. Chem. Soc.* **143**, 2005–2015 (2021).
47. Guo, L. et al. General method for enantioselective three-component carboarylation of alkenes enabled by visible-light dual photoredox/nickel catalysis. *J. Am. Chem. Soc.* **142**, 20390–20399 (2020).
48. Cong, F., Lv, X.-Y., Day, C. S. & Martin, R. Dual catalytic strategy for forging sp^2–sp^3 and sp^3–sp^3 architectures via β-scission of aliphatic alcohol derivatives. *J. Am. Chem. Soc.* **142**, 20594–20599 (2020).
49. Li, Y. et al. Highly selective synthesis of all-carbon tetrasubstituted alkenes by deoxygenative alkenylation of carboxylic acids. *Nat. Commun.* **13**, 10 (2022).
50. Li, J., Luo, Y., Cheo, H. W., Lan, Y. & Wu, J. Photoredox-catalysis-modulated, nickel-catalyzed divergent difunctionalization of ethylene. *Chem.* **5**, 192–203 (2019).
51. Welin, E. R., Le, C., Arias-Rotondo, D. M., McCusker, J. K. & MacMillan, D. W. C. Photosensitized, energy transfer-mediated organometallic catalysis through electronically excited nickel(II). *Science* **355**, 380–385 (2017).
52. Heitz, D. R., Tellis, J. C. & Molander, G. A. Photochemical nickel-catalyzed C–H arylation: synthetic scope and mechanistic investigations. *J. Am. Chem. Soc.* **138**, 12715–12718 (2016).
53. Xuan, J. et al. Visible-light-induced formal [3+2] cycloaddition for pyrrolesynthesis under metal-free conditions. *Angew. Chem. Int. Ed.* **53**, 5653–5656 (2014).
54. Chatterjee, A. & König, B. Birch-type photoreduction of arenes and heteroarenes by sensitized electron transfer. *Angew. Chem. Int. Ed.* **58**, 14289–14294 (2019).
55. Metternich, J. B. & Gilmour, R. One photocatalyst, *n* activation modes strategy for cascade catalysis: emulating coumarin biosynthesis with (−)-riboflavin. *J. Am. Chem. Soc.* **138**, 1040–1045 (2016).
56. Singh, A., Fennell, C. J. & Weaver, J. D. Photocatalyst size controls electron and energy transfer: selectable *E*/*Z* isomer synthesis via C–F alkenylation. *Chem. Sci.* **7**, 6796–6802 (2016).
57. Zhu, C. et al. A multicomponent synthesis of stereodefined olefins via nickel catalysis and single electron/triplet energy transfer. *Nat. Catal.* **2**, 678–687 (2019).
58. Guo, L., Song, F., Zhu, S., Li, H. & Chu, L. *syn*-Selective alkylarylation of terminal alkynes via the combination of photoredox and nickel catalysis. *Nat. Commun.* **9**, 4543 (2018).
59. Großkopf, J., Kratz, T., Rigotti, T. & Bach, T. Enantioselective photochemical reactions enabled by triplet energy transfer. *Chem. Rev.* **122**, 1626–1653 (2022).
60. Teders, M. et al. The energy-transfer-enabled biocompatible disulfide–ene reaction. *Nat. Chem.* **10**, 981–988 (2018).
61. Chinn, A. J., Sedillo, K. & Doyle, A. G. Phosphine/photoredox catalyzed anti markovnikov hydroamination of olefins with primary sulfonamides via α-scission from phosphoranyl radicals. *J. Am. Chem. Soc.* **143**, 18331–18338 (2021).
62. Na, C. G., Ravelli, D. & Alexanian, E. J. Direct decarboxylative functionalization of carboxylic acids via O–H hydrogen atom transfer. *J. Am. Chem. Soc.* **142**, 44–49 (2020).
63. Fawcett, A. et al. Photoinduced decarboxylativeborylation of carboxylic acids. *Science* **357**, 283–286 (2017).
64. Pitzer, L., Schäfers, F. & Glorius, F. Rapid assessment of the reaction-condition-based sensitivity of chemical transformations. *Angew. Chem. Int. Ed.* **58**, 8572–8576 (2019).
65. Gensch, T., Teders, M. & Glorius, F. Approach to comparing the functional group tolerance of reactions. *J. Org. Chem.* **82**, 9154–9159 (2017).
66. Strieth-Kalthoff, F. & Glorius, F. Triplet energy transfer photocatalysis: unlocking the next level. *Chem* **6**, 1888–1903 (2020).
67. Müller, C., Pascher, T., Eriksson, A., Chabera, P. & Uhlig, J. KiMoPack: a Python package for kinetic modeling of the chemical mechanism. *J. Phys. Chem. A* **126**, 4087–4099 (2022).
68. Lowry, M. S. et al. Single-layer electroluminescent devices and photoinduced hydrogen production from an ionic iridium(III) complex. *Chem. Mater.* **17**, 5712–5719 (2005).
69. Ohkubo, K., Nanjo, T. & Fukuzumi, S. Photocatalytic electron transfer oxidation of triphenylphosphine and benzylamine with molecular oxygen via formation of radical cations and superoxide ion. *Bull. Chem. Soc. Jpn* **79**, 1489–1500 (2006).
70. Tojo, S., Yasui, S., Fujitsuka, M. & Majima, T. Reactivity of triarylphosphine peroxyl radical cations generated through the reaction of triarylphosphine radical cations with oxygen. *J. Org. Chem.* **71**, 8227–8232 (2006).
71. Boeré, R. T. et al. Photophysical, dynamic and redox behavior of tris(2,6-diisopropylphenyl)phosphine. *New J. Chem.* **32**, 214–231 (2008).

72. Stache, E. E., Ertel, A. B., Rovis, T. & Doyle, A. G. Generation of phosphoranyl radicals via photoredox catalysis enables voltage-independent activation of strong C–O bonds. *ACS Catal.* **8**, 11134–11139 (2018).
73. Zhang, M., Xie, J. & Zhu, C. A general deoxygenation approach for synthesis of ketones from aromatic carboxylic acids and alkenes. *Nat. Commun.* **9**, 3517 (2018).
74. Zhang, M., Yuan, X.-A., Zhu, C. & Xie, J. Deoxygenative deuteration of carboxylic acids with D_2O. *Angew. Chem. Int. Ed.* **58**, 312–316 (2019).
75. Ning, Y. et al. Site-specific Umpolung amidation of carboxylic acids via triplet synergistic catalysis. *Nat. Commun.* **12**, 4637 (2021).
76. Pan, X. et al. Mechanism of photoinduced metal-free atom transfer radical polymerization: experimental and computational studies. *J. Am. Chem. Soc.* **138**, 2411–2425 (2016).
77. Tokuyama, H., Miyazaki, T., Yokoshima, S. & Fukuyama, T. A novel palladium-catalyzed coupling of thiol esters with 1-alkynes. *Synlett* **10**, 1512–1514 (2003).
78. Ochiai, H., Uetake, Y., Niwa, T. & Hosoya, T. Rhodium-catalyzed decarbonylative borylation of aromatic thioesters for facile diversification of aromatic carboxylic acids. *Angew. Chem. Int. Ed.* **56**, 2482–2486 (2017).
79. Wenkert, E. & Chianelli, D. J. Nickel-catalysed decarbonylation of thioesters. *J. Chem. Soc., Chem. Commun.*, 627–628 (1991).

Acknowledgements

We thank Y. Li (Wuhan University) and S. Dutta (WWU) for helpful discussions. X.Q. acknowledges the National Natural Science Foundation of China (no. 22201222) and the supercomputing system in the Supercomputing Center of Wuhan University. Generous financial support by the Alexander von Humboldt Foundation, the Deutsche Forschungsgemeinschaft (Leibniz Award) and the International Graduate School for Battery Chemistry, Characterization, Analysis, Recycling and Application (BACCARA), funded by the Ministry for Culture and Science of North Rhine Westphalia, Germany.

Author contributions

H.W., A.D., P.B. and F.G. designed, performed and analysed experiments. Z.L. and X.Q. performed the DFT calculation. S.M. and F.T. performed and analysed the transient absorption spectroscopy. H.W., X.Q and F.G. prepared the paper with contribution from all authors. All the authors discussed the results and commented on the paper.

Funding

Open access funding provided by Westfälische Wilhelms-Universität Münster.

Competing interests

The authors declare no competing interests.

Additional information

Supplementary information The online version contains supplementary material available at https://doi.org/10.1038/s44160-023-00353-z.

Correspondence and requests for materials should be addressed to Friedrich Temps, Xiaotian Qi or Frank Glorius.

Peer review information *Nature Synthesis* thanks the anonymous reviewers for their contribution to the peer review of this work. Primary Handling Editor: Thomas West, in collaboration with the *Nature Synthesis* team.